◆ Human Brain Mapping 34:3280–3298 (2013) ◆

Short-Time Windows of Correlation Between Large-Scale Functional Brain Networks Predict Vigilance Intraindividually and Interindividually

Garth John Thompson,[1] Matthew Evan Magnuson,[1] Michael Donelyn Merritt,[1] Hillary Schwarb,[2] Wen-Ju Pan,[1] Andrew McKinley,[3] Lloyd D. Tripp,[3] Eric H. Schumacher,[2] and Shella Dawn Keilholz[1]*

[1]*Biomedical Engineering, Georgia Institute of Technology and Emory University, Atlanta, Georgia*
[2]*School of Psychology, Georgia Institute of Technology, Atlanta, Georgia*
[3]*Air Force Research Laboratory, Wright-Patterson Air Force Base, Ohio*

Abstract: A better understanding of how behavioral performance emerges from interacting brain systems may come from analysis of functional networks using functional magnetic resonance imaging. Recent studies comparing such networks with human behavior have begun to identify these relationships, but few have used a time scale small enough to relate their findings to variation within a single individual's behavior. In the present experiment we examined the relationship between a psychomotor vigilance task and the interacting default mode and task positive networks. Two time-localized comparative metrics were calculated: difference between the two networks' signals at various time points around each instance of the stimulus (peristimulus times) and correlation within a 12.3-s window centered at each peristimulus time. Correlation between networks was also calculated within entire resting-state functional imaging runs from the same individuals. These metrics were compared with response speed on both an intraindividual and an interindividual basis. In most cases, a greater difference or more anticorrelation between networks was significantly related to faster performance. While interindividual analysis showed this result generally, using intraindividual analysis it was isolated to peristimulus times 4 to 8 s before the detected target. Within that peristimulus time span, the effect was stronger for individuals who tended to have faster response times. These results suggest that the relationship between functional networks and behavior can be better understood by using shorter time windows and also by considering both intraindividual and interindividual variability. *Hum Brain Mapp 34:3280–3298, 2013.*

Key words: functional connectivity; default mode; task positive; large scale cerebral networks; psychomotor vigilance task; pvt; spontaneous fluctuations; resting state; windowed correlation; performance prediction

Additional Supporting Information may be found in the online version of this article.

Contract grant sponsor: Bio-nano-enabled Inorganic/Organic Nanostructures and Improved Cognition (BIONIC) Air Force Center of Excellence at the Georgia Institute of Technology.

*Correspondence to: Shella Dawn Keilholz, Biomedical Engineering, Emory University, 101 Woodruff Circle WMB 2001, Atlanta, GA 30322. E-mail: shella.keilholz@bme.gatech.edu

Received for publication 24 June 2011; Revised 22 March 2012; Accepted 14 May 2012

DOI: 10.1002/hbm.22140

Published online 27 June 2012 in Wiley Online Library (wileyonlinelibrary.com).

INTRODUCTION

One critical question for cognitive neuroscience is: how do cognitive processes and behavioral performance emerge from interacting brain systems? Originally demonstrated by Biswal et al. [1995], spontaneous low frequency oscillations appear to be correlated in anatomically connected regions [Fox et al., 2006; Hampson et al., 2002; Raichle et al., 2001]. Techniques that identify these regions, known as functional connectivity, map the brain's functional networks [Calhoun et al., 2001; Cordes et al., 2000] which exist even when an individual is not performing a task, referred to as the resting state [Raichle et al., 2001]. Variation in functional networks was initially investigated in the context of Alzheimer's disease [Greicius et al., 2004; Rombouts et al., 2005] but has since been applied to prediction of behavioral variability in healthy individuals performing tasks. Tasks studied have included working memory [Hampson et al., 2006; Tambini et al., 2010; Wang et al., 2010], motor learning [Albert et al., 2009], language [Hasson et al., 2009; Waites et al., 2005], executive control or maintenance of attention against distractions [Eichele et al., 2008; Kelly et al., 2008; Prado et al., 2011; Prado and Weissman, 2011a,b; Seeley et al., 2007; Weissman et al., 2006], and auditory or somatosensory stimulus detection [Boly et al., 2008; Sadaghiani et al., 2009]. These studies' results support the hypothesis that functional networks and the associated BOLD signal are linked to cognitive processing.

Though the majority of studies use similar functional magnetic resonance imaging (fMRI) protocols, the functional network metrics extracted from these data vary [Hampson et al., 2006; Kelly et al., 2008; Prado and Weissman, 2011a; Seeley et al., 2007; Waites et al., 2005; Weissman et al., 2006]. In general, only a few studies, examining mean signal within networks over time, have considered the temporal evolution of functional connectivity before and after performance of the task [Boly et al., 2008; Eichele et al., 2008; Sadaghiani et al., 2009; Weissman et al., 2006]. In a recent review by Sadaghiani et al. [2010] it was noted that both the type of task and the time point around the instance of the stimulus (peristimulus time) affect how the signal in the network will be related to performance. This matches what is seen in models of spontaneous brain activity which suggest that the correlated/anticorrelated networks seen are due to the spatiotemporal structure of activity rather than a direct agonistic/antagonistic relationship; for a recent review see Deco et al. [2011]. Such results suggest that functional network activity on a scale of seconds may contain information about cognition; information that may be lost when longer time scales are used.

While the majority of studies have used one or more entire fMRI runs, typically 6 to 10 min, to calculate correlation values (or independent components, etc.) [Albert et al., 2009; Hampson et al., 2006; Hasson et al., 2009; Kelly et al., 2008; Seeley et al., 2007; Tambini et al., 2010; Waites et al., 2005; Wang et al., 2010], notable exceptions exist. Chang and Glover [2010] illustrated that dominant frequency within networks changes on a scale of tens of seconds or less. A resting-state study by Majeed et al. [2011] demonstrated highly reproducible spatiotemporal dynamics in the low-frequency BOLD signal. A similar pattern on a similar time scale was observed by Grigg and Grady [2010], who claimed it as one of two fundamental states of a network known as the default mode network. At least two studies have examined functional connectivity in 30-s windows and suggested that it may be more diagnostic than functional connectivity calculated from entire fMRI runs [Honey et al., 2007; Sakoglu et al., 2010]. The overall impression is that the time scales involved (including the window lengths used) in functional network analysis could be much shorter.

The present experiment set out to apply both traditional functional connectivity (using entire functional imaging runs to calculate correlation) and short-window correlation methods to performance prediction in healthy individuals both across the group (interindividually) and approximating per-individual results (intraindividually). The time windows used in the windowed correlation analysis were short enough to only reflect momentary, second-scale differences such as those seen by Majeed et al. [2011].

The psychomotor vigilance task (PVT) [Dinges and Powell, 1985] was chosen for this study because it is a measure of sustained attention and both the default mode network and regions related to attentional control (i.e., the task positive network) [Lim and Dinges, 2008] are known to be involved. Using fMRI and the general linear model to study the PVT, Drummond et al. [2005] demonstrated that optimal performance was associated with a greater response in regions associated with sustained attention (e.g. inferior parietal and premotor cortex) whereas suboptimal performance was associated with activity in the default mode network (e.g. posterior cingulate and medial frontal cortex). Both the default mode network and the task positive network, which overlaps with attentional control networks [Fox et al., 2005; Fransson, 2005], were involved in the second-scale activity observed by Chang and Glover [2010] and Majeed et al. [2011]. Additionally, the default mode network deactivates in response to task performance on time scales as short as only a few seconds [Singh and Fawcett, 2008]. Such results suggest dynamic properties of both the default mode and task positive networks, and that dynamic interaction between these networks may be responsible for performance variation in the PVT.

In the present study we compare functional connectivity metrics on different time scales (an entire fMRI run, a 12.3-s window or a single data point) with multiple statistical interpretations of reaction time (interindividual linear regression and two-group analysis using interindividual and intraindividual separations). Knowledge of which functional connectivity metrics predict fast PVT performance will demonstrate if short-time scale analysis can be used to produce similar results to traditional entire-run

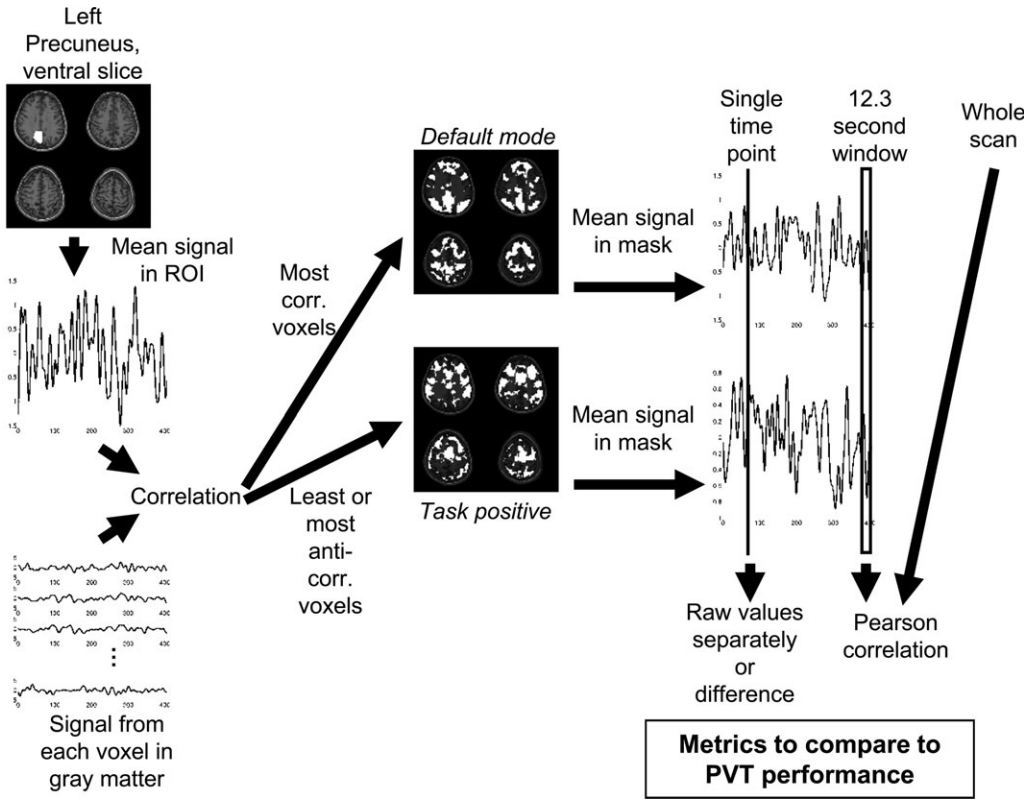

Figure 1.

Calculation of functional connectivity metrics to compare to PVT performance. To calculate metrics from functional connectivity to compare with PVT performance, masks are generated from Pearson product-moment correlation coefficient (*r*) and then the mean signal is compared. The left precuneus in the most ventral image slice is found as an ROI using SPM8 and marsbar (shown in white). The mean signal in this ROI is taken and *r* calculated between it and every voxel in gray matter. The 1,639 (10% of whole image) voxels in gray matter most correlated with the ROI are taken as the default mode network (shown in white). The 1,639 voxels least correlated or most anticorrelated with the ROI in gray matter are taken as the task positive network (shown in white). The mean signal in each network mask is taken to produce a default mode network signal and a task positive network signal. The network signals are compared in several manners. At a single time point at some shift relative to an instance of PVT performance the mean signal in both networks and the difference in signal between networks can be compared to performance. In a 12.3-s window at some peristimulus time relative to an instance of PVT performance, *r* between the two networks' mean signals can be calculated and compared with performance. Finally *r* between the entireties of the two networks' signals from each functional imaging run can be compared to performance.

functional connectivity. Furthermore, comparing intraindividual performance with functional connectivity will suggest whether performance prediction can be analyzed on a per individual basis or can only be analyzed using a group. We aspire to motivate future work to both consider shorter time scales for functional connectivity analysis and the possibility of using intraindividual variations in functional connectivity to predict performance.

MATERIALS AND METHODS

A brief summary of the methods used can be found in Figure 1 and Table I.

Data Collection

Seventeen healthy human individuals were recruited (nine males and eight females) with an age range of 18 to 26 years. Informed consent was obtained from all individuals. All studies were performed in compliance with the Georgia Institute of Technology Institutional Review Board. All data were acquired at the joint Georgia Institute of Technology/Georgia State University Center for Advanced Brain Imaging.

All 17 individuals underwent high temporal resolution fMRI while performing a PVT. In this task participants fixated on a centrally presented black dot subtending 0.28° of visual angle on a gray background. When the dot changed

TABLE I. Example of calculation of intraindividual and interindividual human performance metrics from PVT reaction times

	Individual 1 (ms)	Individual 2 (ms)	Individual 3 (ms)
Overall median			
Instances classified as "fast"	942; 1,029	716; 693; 648	920
Instances classified as "slow"	1,054; 1,329	1,331	1,204; 1,156; 1,314
Individuals' own medians			
Instances classified as "fast"	942; 1,029	693; 648	920; 1,156
Instances classified as "slow"	1,054; 1329	716; 1,331	1,204; 1,314

Each individual has several instances of the PVT which, for testing purposes, are divided into fast and slow groups in two manners. An overall median is calculated for all performance times from all individuals. In this example, it is 1,041.5 ms. Each individual's reaction times are classified as fast or slow based upon being less than or greater than this median, respectively. This metric can be compared with all predictive metrics calculated from functional connectivity in this study. The groups of fast and slow reaction times can be considered interindividual differences. Each individual has a median calculated separately. Each individual's own reaction times are classified as fast or slow based upon being less than or greater than these individual median values, respectively. In this case, each individual has approximately 50% fast and 50% slow reaction times. This metric can be used to classify performance using a functional connectivity metric calculated at some peristimulus time around performance but (in the present study) cannot be used to classify performance using resting-state functional connectivity. The groups of fast and slow reaction times can be considered intraindividual differences.

to navy blue, participants pressed a button with their right index finger as quickly as possible. If participants failed to respond in 9 s, the dot returned to black. Each block lasted 8 min and the dot changed color between three and five times. Change onset was random for each participant (the delay time between onsets as an integer number of milliseconds randomly chosen from a range of 10,000 ms to 480,000 ms without replacement). Four fMRI runs of PVT performance were collected from each individual. Two fMRI resting-state runs were collected from each individual. In resting-state runs, individuals were told to lie quietly. The order of runs was counterbalanced between two options (Option 1: resting state, two PVT, resting state and two PVT. Option 2: two PVT, resting state, two PVT and resting state). In resting-state runs individuals fixated on the black dot, but it never changed to navy blue. Participants were always informed that no change would occur before the start of each resting-state run.

Functional images were acquired using echo planar imaging (EPI) from four horizontal slices with voxels of size 3.4 mm in the frequency and phase encoding directions and 5 mm in the slice direction, repetition time (TR) 300 ms, echo time (TE) 30 ms, and 1600 images. Slices were manually positioned to include the precuneus, medial prefrontal cortex, inferior parietal cortex, and angular gyri using Figure 3 from Fox et al. [2005; p 9679] as reference. Structural images were acquired using a T1-weighted MP RAGE 3D sequence with 1 mm isotropic voxels.

Data Preprocessing

The following preprocessing steps were done in Statistical Parametric Mapping 8 (SPM8) using the marsbar region of interest (ROI) plug-in: T1 images were segmented into gray matter, white matter, and cerebrospinal fluid maps. The left precuneus ROI from the AAL Structural ROI library [Brett, 2002] was reverse normalized [Chang and Glover, 2010] from the MNI brain template to the individual T1 images. Individual T1 images were spatially cropped and registered to same-individual EPI images and this transformation was applied to all segments and left precuneus ROI as well. Reverse normalization allowed analysis to be performed in individual space rather than normalized space. This was necessary because individual EPI images did not cover the whole brain and had decreased signal-to-noise ratio due to the short TR used in this study.

EPI data were first slice-time corrected and then motion corrected through registration to a mean of all EPI images using Analysis of Functional NeuroImages (AFNI). From AFNI the maximum total movement in each direction (X, Y, and Z) was recorded; 100 TR (30 s) were removed from the beginning of EPI and motion data to eliminate stabilization effects. EPI data were blurred with a spatial Gaussian with sigma of $2 \times 2 \times 1$ voxels and size of $3 \times 3 \times 1$ voxels. A finite impulse response filter was used with a length of 150 TR (45 s) and a pass band of 0.01 to 0.08 Hz. As behavioral onset times were recorded in milliseconds from the start of the functional imaging run in raw data, they were corrected for the removed TRs and the phase shift resulting from the filter. Each voxel within EPI data was quadratically de-trended [Majeed et al., 2011] and divided by one standard deviation, resulting in unit variance. Mean signals were calculated for whole-brain and white matter and these signals, in addition to filtered and cropped motion parameter signals, were regressed from EPI data. Final EPI data were again set to zero mean and unit variance for each voxel. This produced a normalized BOLD signal.

As it is debatable what to expect for a hemodynamic response to spontaneous fluctuations [Logothetis et al., 2009; Shmuel and Leopold, 2008], the normalized BOLD signal was not de-convolved with any hemodynamic

response function. To compensate for this the central time point was placed at a delay of 4 s rather than 0 s [Miezin et al., 2000, see "prediction using signal change" below).

Functional Network Generation

For each normalized EPI time-course (405 s after cropping and filtering) masks for default mode network and task positive network were created. The left precuneus ROI in the most ventral image slice was chosen as a seed region as it is a large, easily identified component of the default mode network [Fox et al., 2005; Fransson, 2005]. The left side was chosen arbitrarily. The Pearson product-moment correlation coefficient (r) was calculated between the mean normalized time course for the seed region and each voxel's normalized time course for the entire fMRI run.

The 1,639 voxels in gray matter with the highest positive correlation with the precuneus were taken as the default mode network. The 1,639 voxels in gray matter with the weakest positive or strongest negative correlation were taken as the task positive network. A constant number of voxels was chosen to maintain constant signal-to-noise ratio for mean signals from voxels within each network. The number 1,639 was 10% of the total number of voxels in the image (ceiling of $0.1 \times 64 \times 64 \times 4$). Percentiles of 5, 10, 15, 20, and 30 were tried and 10% was a sufficient number of voxels to produce default mode maps that appeared consistent to those presented by Fransson [2005] when plotted against T1-weighted anatomical images. Functional imaging runs where the gray matter did not have at least 1,639 voxels were excluded, but otherwise no exclusivity was enforced for any voxel across different networks or fMRI runs. For each individual and functional imaging run a mean time course was taken from each of these networks to produce a default mode network signal and a task positive network signal.

Exclusion

Functional imaging runs were excluded if the total range of movement in any direction was greater than the size of a voxel in the phase or frequency encoding direction (3.4 mm). However, functional imaging runs excluded due to motion or mask parameters were not excluded for calculation of behavioral parameters. Furthermore, instances where the individual failed to respond within 9 s were recorded as failures and excluded from both BOLD and behavioral data analysis.

Classification into Fast and Slow Responses

While reaction times theoretically are continuously variable, for comparison with previous studies examining spontaneous fluctuations temporally locked to task performance it is desirable to divide reaction times into two groups of good performance (here, fast performance) and bad performance (here, slow performance) on the PVT [Boly et al., 2008; Eichele et al., 2008; Sadaghiani et al., 2009; Weissman et al., 2006]. Dividing instances into fast response and slow response groups also allows the characteristic spontaneous activity for fast response instances and for slow response instances to be examined separately.

Two performance metrics are desired: one which relates to variation within an individual's own performance, and a different metric which considers the entire group. To this end, instances of change onset, when the circle changed color from black to navy blue and the individual responded, were classified into fast response and slow response groups based on two metrics.

The first interindividual metric was calculated by identifying the overall median value for all 17 individuals' response times combined. Instances were grouped into a fast response group and a slow response group whether the response time fell below or above this overall median, respectively. Data falling into the central 5% of response times was excluded from this analysis to ensure separation between the two groups.

The second intraindividual metric was identical, except the median value to which any given instance was compared was calculated only using instances from the specific individual to which that instance belonged. Therefore individuals' instances were only compared with their own reaction times and each individual had approximately 50% of reaction times classified as fast and 50% as slow. Table I shows an example of each metric.

Prediction Using Comparative Metrics

Two comparative metrics (short-window correlation and local difference in magnitude) were chosen for their ability to extract a time-localized relationship between activity in the default mode network and the task positive network. Such metrics would thus target the time scale of the spatiotemporal dynamics of the default mode and task positive networks which have been observed to have phase differences between networks on a scale of seconds [Grigg and Grady, 2010; Majeed et al., 2011]. These metrics are described more fully in their own sections below.

Both metrics were calculated at time locations from 16 s before to 24 s after each instance of the task. The time difference between the stimulus and the time location where the metric was calculated is referred to as the peristimulus time [Boly et al., 2008; Sadaghiani et al., 2009, 2010]. Peristimulus times was centered at 4 s, which is the expected peak hemodynamic response in the motor cortex to a simple visual stimulation motor response task [Miezin et al., 2000]. This interval also ensures with 95% confidence that no other change onset occurred at a peristimulus time that would be analyzed for the current onset, and is a large enough time span to compare with results seen in analysis

of similar tasks, such as the flanker task which also measures attention, though in terms of cognitive control rather than maintenance [Eichele et al., 2008; see discussion). If the peristimulus time was such that it fell outside of available normalized BOLD data, then that peristimulus time was excluded from analysis for that instance.

Each metric at each peristimulus time was compared with reaction time in two manners. First, a linear regression was performed between the value of the metric and reaction time, producing an R^2 value, slope and slope standard error. Based on the slope and its standard error a P value was calculated (assuming a T distribution) and this was used as a probability of null hypothesis. The resulting 42 P values (21 time points, correlation, and magnitude) were tested to control family-wise error rate (see below). This method has higher statistical power as every point is used, but can only look at interindividual differences due to the limited number of points per individual in this study.

Second, fast response and slow response groups were compared using a two-sample t-test at every peristimulus time. The resulting 84 P values (21 time points, overall and own medians, correlation, and magnitude) were tested to control family-wise error rate (see below). This method has lower statistical power but allows comparison of intraindividual and interindividual differences. Two-group statistical testing may produce different results than linear testing, e.g. one group may follow a linear trend but show no difference in mean when compared with the other group.

Short-Window Correlation

As frequencies above 0.08 Hz were greatly attenuated by filtering, r in a window shorter than 12.5 s (1/0.08 Hz = 12.5 s) reflected only similarity in time-local magnitude. Here 41 TRs (41 × 0.300 s = 12.3 s) were chosen for the correlation window as 12.3 s < 12.5 s.

Local Difference in Magnitude

If the mean signal from the task positive network is subtracted from the mean signal from the default mode network it provides a measure of the current relationship between the two networks. This was calculated point-by-point on normalized data.

Intraindividual Prediction Within Fast and Slow Groups

Individuals were separated into a fast individuals group and a slow individuals group depending upon whether an individual's own median response time was above or below the overall median response time. Response instances from all individuals in each group (fast individuals and slow individuals) were then divided into fast and slow response instances based upon each individual's own median response time as described above (see Table I for an example) to approximate intraindividual performance.

As statistical power was greatly reduced by separating individuals into fast and slow groups, a reduced number of peristimulus times were used. Only peristimulus times found to be significant using either of the intraindividual two-group metrics (see section Intraindividual prediction using comparative metrics in Results and Fig. 6) were used.

At each remaining peristimulus time, the short-window correlation and local difference in magnitude metrics (see above) were calculated. The fast response instances for each metric (short-window correlation and local difference in magnitude) and each set of individuals (fast individuals and slow individuals) were compared with the slow response instances for the same metric and set of individuals using a two-sample t-test at every peristimulus time. Family-wise error rate control was used on the fast individuals group and the slow individuals group separately with six hypotheses in each family (three time points, short-window correlation and local difference in magnitude).

Resting-State Correlation

For comparison with the many functional connectivity studies on the time scale of entire fMRI runs [Albert et al., 2009; Hasson et al., 2009; Kelly et al., 2008; Tambini et al., 2010; Waites et al., 2005; Wang et al., 2010], r was calculated between the mean normalized BOLD signal within the default mode network and the task positive network for the entirety of each individual's resting-state functional imaging runs. Each resulting correlation value was used as a data point compared with whether an individual's own median response time was above or below the overall median response time. This was tested with a two-sample t-test. This was done to assess the relationship between network interaction and performance on an interindividual, entire-functional-imaging-run basis. No family-wise error rate control was performed.

Family-Wise Error Rate Control

The purpose of this study was data-driven: to identify functional network properties predictive of individual performance rather than to model all such possible factors. Therefore, the results include multiple hypotheses, each represented by a probability (P value). Hypotheses are separated into families based on similarity in purpose as shown in Table II.

As multiple P values resulting from multiple hypotheses are calculated, it was necessary to control against Type I statistical errors (false positives). In this study the family-wise error rate (FWER) was chosen instead of false

TABLE II. Statistical families

Mask creation	Metric type	Test type	SGoF significance	Family number
Entire run	Masks	Two group	None	1
Entire run	Mag. dif. and 12.3 s *r*	Linear	≤0.05	2
Entire run	Mag. dif. and 12.3 s *r*	Two group	≤0.005	3
Entire run	Mag. dif. and 12.3 s *r*	Two group, Fast	≤0.005	4
Entire run	Mag. dif. and 12.3 s *r*	Two group, Slow	≤0.05	5
Entire run	DMN and TPN	Linear	≤0.005	6
Entire run	DMN and TPN	Two group	None	7
12.3 s window	Masks	Two group	≤0.05[a]	8
12.3 s window	Mag.dif. and 12.3 s *r*	Linear	≤0.005	9
12.3 s window	Mag.dif. and 12.3 s *r*	Two group	≤0.005	10
12.3 s window	DMN and TPN	Linear	≤0.1	11
12.3 s window	DMN and TPN	Two group	None	12

The 12 statistical families used in this study. Each family was tested separately to control family-wise error rate (FWER). Each statistical family also had a control calculated using randomized onset times, except for families 1 and 8 where the data with randomized onset times was instead used to calculate bootstrapping significance cutoffs (see Supporting Information). As only one hypothesis was tested for resting-state data, it is not considered a "family." See Table SI in Supporting Information for more details. The columns include: mask creation: method of creating default mode and task positive network masks. Either the entire fMRI run or a 12.3 s window centered on the peristimulus time was used. Metric type: "masks" is comparison between the probability of a voxel occurring in a fast performance group's masks and a slow performance group's masks. Mag. dif. is difference in magnitude between the default mode and task positive networks' mean signals at the peristimulus time; 12.3 s *r* is correlation between the default mode and task positive networks' signals in a window of 12.3 s centered at the peristimulus time. DMN (default mode network) and TPN (task positive network) is the mean signal in that network at the peristimulus time. Test type: "two group" is where instances of task performance were divided into two groups for comparison, in both an interindividual and an intraindividual manner. "Linear" is where metrics were compared with reaction time using linear regression. "Fast" or "slow" indicates that only individuals either faster than or slower than the overall median reaction time were used. SGoF significance: with the exception of the "Mask" metric, significance was tested using SGoF correction for FWER at 0.05, 0.1, and 0.005. The lowest probability cutoff where significance was found is shown, or "none" if no results passed SGoF correction at 0.05 FWER. Family number: reference numbers for each statistical family.
[a]The mask metric was tested using only 0.05.

discovery rate as it detects families of viable hypotheses instead of testing hypotheses on an individual basis.

The sequential goodness of fit (SGoF) method was used to control FWER at 5% chance that all rejected null hypotheses are false positives [Carvajal-Rodriguez et al., 2009]. SGoF performs an exact binomial test onto the expected distribution of *P* values under the complete null hypothesis (no results significant). Therefore unlike standard Bonferroni FWER correction, SGoF will not increase in Type II error (false negative) rate as the number of *P* values tested increases.

As SGoF assumes comparisons are independent, and comparisons in this study are likely to be nonindependent, the possibility exists that this nonindependence will create a cluster of small *P* values which will be incorrectly reported as significant. Therefore standard Bonferroni correction, which decreases the chance of reporting significance if comparisons are correlated, was also performed. Bonferroni correction has a high Type II error rate, so not all hypotheses found to be significant by SGoF are expected to be found significant by Bonferroni. However, if any hypotheses are significant by Bonferroni it suggests SGoFs results are not due to clustering randomly small *P* values.

As SGoF uses the distribution of *P* values to calculate significance it does not automatically consider a *P* value of zero to be significant, unlike Bonferroni. Therefore when *P* values are calculated using bootstrapping (see Supporting Information) only SGoF will be used.

Control

The type of functional imaging run (resting state vs. PVT), change onsets and response times were randomly permuted between all functional imaging runs and all subjects. These randomly permuted behavioral data were compared with original-order BOLD data using the signal change and comparative metrics. Other than randomization of behavioral data, analysis was identical to the descriptions above and in Supporting Information, including separate control of family-wise error rate for each family of hypotheses.

Table II illustrates the 12 families of hypotheses that were included in this study. Excluding families 1 and 8, 10 families had a control significance test performed. From 10 families, it is likely (40.1% chance, from binomial distribution) that at least one will show a false positive, but less than 5% likely (1.15%, from binomial distribution) that three will show a false positive. Therefore if more than three control tests show a false positive, it suggests that there was a methodological error in significance testing.

RESULTS

Twenty-two functional imaging runs were removed due to excess motion, resulting in exclusion of two individuals. One functional imaging run was removed due to the required network size being larger than the entirety of gray matter, preventing the creation of network masks. The final number of functional imaging runs was 45 (from 68) over 15 individuals (from 17). Based on the peristimulus time tested, a total of between 131 and 136 instances occurred per usable peristimulus time within these 45 remaining functional imaging runs.

Maps of the default mode and task positive networks were successfully obtained in all functional imaging runs for all remaining individuals. Figure 2 shows probability maps illustrating how often any given voxel was placed within a mask. In Figure 2, all masks were registered using per-slice, rigid-body registration to demonstrate their similarity across subjects (Sochor; available at: http://www.mathworks.com/matlabcentral/fileexchange/19086), though further analysis was performed in individual space. The majority of masks had colocalized regions corresponding to anatomical regions known to be contained within the default mode network (precuneus, angular gyri, and medial prefrontal cortex) and the task-positive network (dorsolateral prefrontal cortex, inferior parietal cortex, and premotor cortex). Masks created from PVT and from resting-state functional imaging runs are similar, suggesting that task performance minimally perturbs the definition of the networks. Figure 3 shows masks created from a single functional imaging run from one individual and the mean BOLD time course within these masks. As expected, these mean time courses are generally anticorrelated (changing in a similar manner but with opposite sign) yet the degree to which they are anticorrelated varies over the functional imaging run [Kelly et al., 2008].

Overall median reaction time was 971 ms; excluding the central 5% of reaction times resulted in instances faster than 939 ms classified as fast and instances slower than 1,014 ms classified as slow. Individual median reaction times varied, with the mean individual median reaction time at 1,060 ms with standard deviation 613 ms. Using an overall median, within the group of fast response instances mean reaction time was 697 ms with standard deviation 125 ms; within the group of slow response instances mean reaction time was 2,001 ms with standard deviation 1,332 ms. Using a median for each individual, within the group of fast response instances mean reaction time was 888 ms with standard deviation 365 ms; within the group of slow response instances mean reaction time was 1,778 ms with standard deviation 1,413 ms.

Figure 4a shows a histogram of reaction times. In Figure 4b these are separated into whether there was positive or negative correlation between the signals from the two networks in a 12.3-s window centered at the change onset (not corrected for hemodynamic response delay). The overall median reaction time of 971 ms is shown as a light dashed line; 971 ms is approximately centered in the large leftmost cluster of reaction times. To the left of 971 ms most bins are dominated by negative correlation, to the right most bins are dominated by positive correlation. These results indicate that median was an appropriate criterion for division of instances.

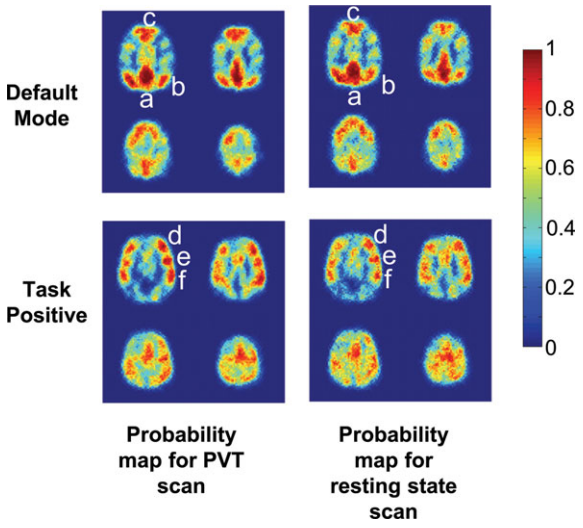

Figure 2.
Probability maps for generated masks. In this study masks were generated on a per-functional-imaging-run basis due to the high temporal resolution EPI used (method shown in Fig. 1). Images shown are four transverse image slices from ventral (upper left) to dorsal (lower right) of human individuals with the nose pointing upwards, nonradiological convention. Masks are registered (for visualization purposes only) using rigid-body registration (Sochor; available at: http://www.mathworks.com/matlabcentral/fileexchange/19086) of co-registered anatomical images on a per-slice basis. Probabilities are shown that any given voxel exists in any given mask of the default mode network or the task positive network, in either the masks generated for PVT or resting-state functional imaging runs. Zero (dark blue) indicates that the voxel never appears in that location, one (dark red) indicates that the voxel always appears in that location, 0.5 (light green) indicates that the voxel appears in half of all masks. The top row shows probabilities for masks generated for the default mode network, the bottom row the task positive network. The first column shows probabilities for masks generated from PVT functional imaging runs, the second column resting-state functional imaging runs. Compare masks with Figure 3 in Fransson [2005]. Anatomical brain locations can be seen for the default mode network corresponding to **(a)** precuneus **(b)** angular gyri **(c)** medial prefrontal cortex, and for the task-positive network corresponding to **(d)** dorsolateral prefrontal cortex, **(e)** premotor cortex, **(f)** inferior parietal cortex.

Interindividual Prediction Using Comparative Metrics

Figure 5 illustrates how comparative metrics relate to interindividual performance at peristimulus times from 16

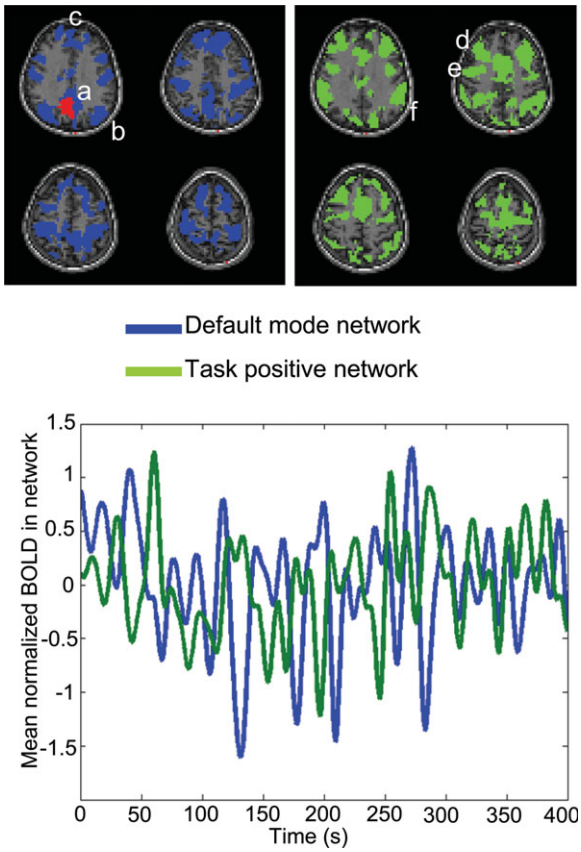

Figure 3.

Example masks and mean time courses. Example masks are shown for the first individual, first PVT functional imaging run. Images shown are four transverse image slices from ventral (upper left) to dorsal (lower right) of one individual with the nose pointing upwards, nonradiological convention. The masks are shown against coregistered anatomical T1-weighted MPrage images. The mask on the left, shown in blue, is for the default-mode network and anatomical brain locations can be seen corresponding to **(a)** precuneus, **(b)** angular gyri, **(c)** medial prefrontal cortex. The ventral left precuneus seed region used to generate these masks is shown in red. The mask on the right, shown in green, is for the task-positive network and anatomical brain locations can be seen corresponding to **(d)** dorsolateral prefrontal cortex, **(e)** premotor cortex, **(f)** inferior parietal cortex. The mean time course from each of these masks is plotted with the mean signal from the default mode network in blue and the mean signal from the task positive network in green. Note that while in general the two signals are anticorrelated, the degree of anticorrelation appears to vary over time [Kelly et al., 2008].

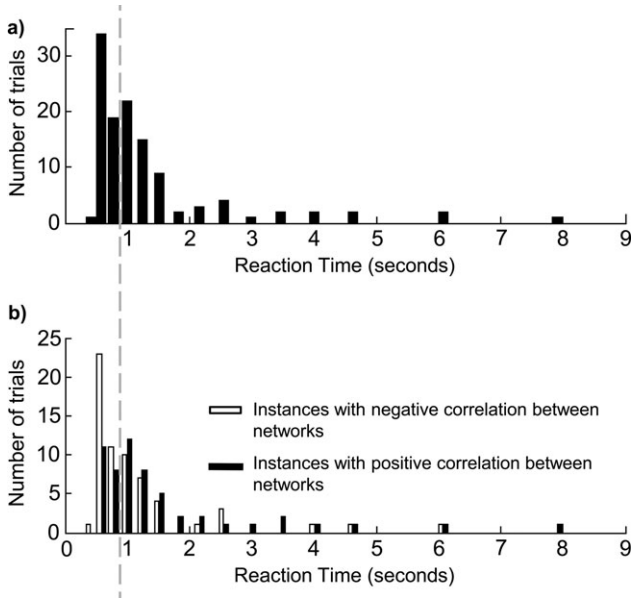

Figure 4.

Histograms of reaction times on PVT. Number of instances of the PVT where individuals responded within a bin of possible reaction times is plotted as a histogram versus the entire possible range of reaction times from 0 s to 9 s. The 20 bin centroids are exponentially distributed from 0 s to 9 s. **(a)** Reaction times are shown together in each bin. **(b)** Each bin is separated into two new bins based upon Pearson product-moment correlation coefficient (r) between the default mode network and the task positive network in a 12.3-s window around the change onset [equivalent to 0 s peristimulus time on Fig. 5b; approximately 4 s before the expected hemodynamic response to neural activity due to task performance, see Miezin et al., 2000] before PVT performance where reaction time was measured. If correlation is negative, the instance is placed in the white bin on the left; if positive the instance is placed in the black bin on the right. The dashed line indicates the overall median reaction time (971 ms). Note that it is centered within the large distribution on the left side of the histogram. Also note that to the left of this median instances with negative correlation between networks dominate, while to the right of this median instances with positive correlation between networks dominate.

s before change onset to 24 s after. The first comparative metric is local difference in magnitude, the signal in the task positive network subtracted from the signal in the default mode network at the peristimulus time around the instance; it is shown in Figure 5a,c. The second comparative metric is short window correlation, which is r in a 12.3-s window centered at the peristimulus time around the instance; it is shown in Figure 5b,d. In Figure 5a,b individual instances are separated into slow and fast response groups by the overall median response time, and the metrics from each group are plotted. Error bars are one standard error. In Figure 5c,d linear regression was performed between the metrics and reaction time (using all response instances), and R^2 values are plotted.

Unlike prediction using signal change (shown in Supporting Information Fig. S1), prediction using comparative metrics (Fig. 5) shows many significant differences before

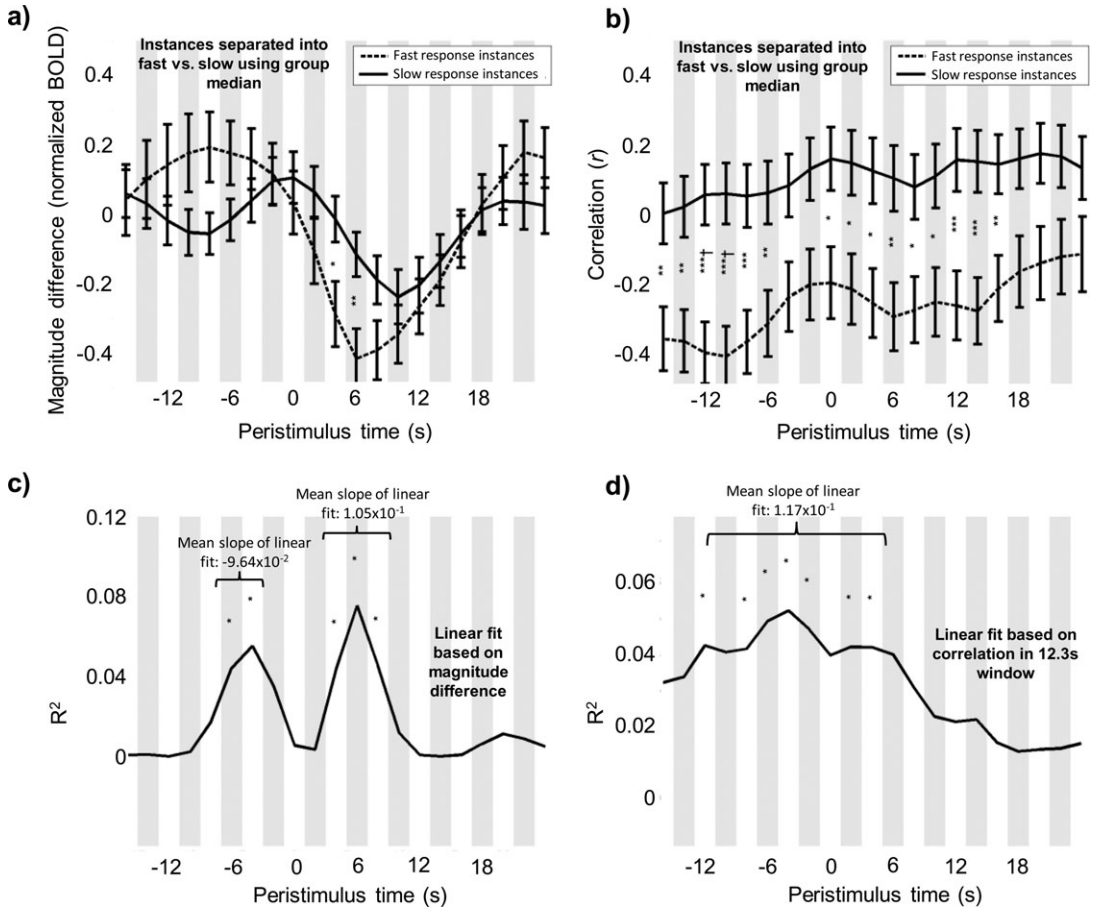

Figure 5.

Interindividual results from comparative metrics. **(a)** Mean signal in default mode network with mean signal in task positive network subtracted from its value. Instances faster than the overall median reaction time are shown as dashed lines; instances slower than the overall median reaction time are shown as solid lines. *X* axis is the amount of time between the calculated value and the change onset cue to perform the task (negative is before task, positive is succeeding task). Error bars are one standard error. **(b)** Pearson product-moment correlation coefficient (*r*) for 12.3 s square window between mean default mode network signal and mean task positive network signal. Instances faster than the overall median reaction time are shown as dashed lines; instances slower than the overall median reaction time are shown as solid lines. *X* axis is the amount of time between the calculated value and the change onset cue to perform the task (negative is before task, positive is succeeding task). Error bars are one standard error. **(c)** R^2 values for linear regression (using all response instances) between reaction time and mean signal in default mode network with mean signal in task positive network subtracted from its value. *X* axis is the amount of time between the calculated value and the change onset cue to perform the task (negative is before task, positive is succeeding task). **(d)** R^2 values for linear regression (using all response instances) between reaction time and Pearson product-moment correlation coefficient (*r*) for 12.3 s square window between mean default mode network signal and mean task positive network signal. *X* axis is the amount of time between the calculated value and the change onset cue to perform the task (negative is before task, positive is succeeding task). Comparisons found to be significant are shown include magnitude difference at peristimulus times of −6 s, −4 s and −4 s to 8 s, correlation at peristimulus times of −16 s to 16 s. They are demarcated as follows: *passes SGoF at 0.05; **passes SGoF at 0.01; ***passes SGoF at 0.005; †passes standard Bonferroni correction at 0.05.

change onset (0 s) or the expected hemodynamic response to neural activity (4 s).

For fast versus slow group analysis, tests passing SGoF correction at 0.05 FWER included: using magnitude difference at peristimulus times of 4 s and 6 s (fast response greater negative difference indicating task positive signal was greater, $P = 1.60 \times 10^{-2}$, 5.36×10^{-3}), and using short-window correlation at peristimulus times of −16 s to −6 s and 0 s to 16 s (fast response greater negative correlation, $3.28 \times 10^{-4} \leq P \leq 1.13 \times 10^{-2}$). Two of these tests passed

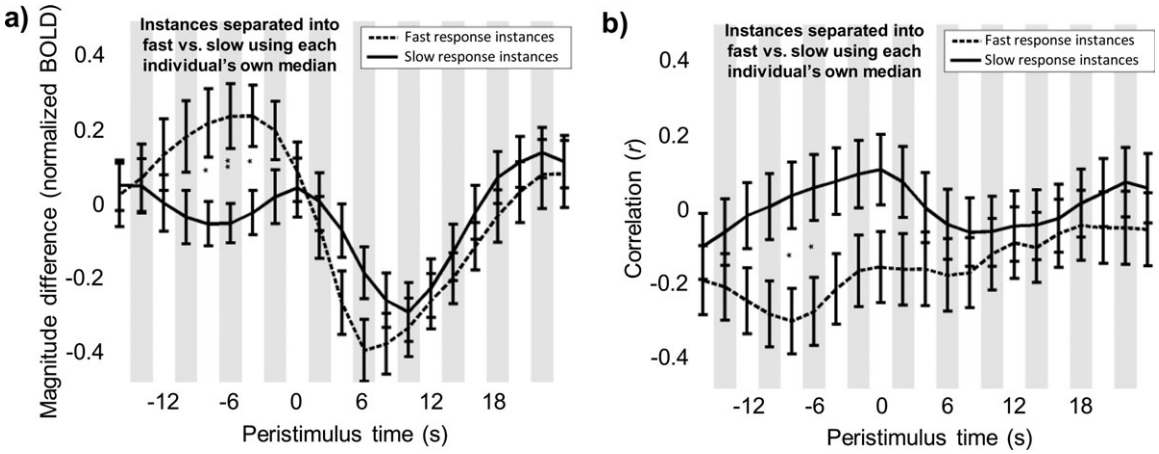

Figure 6.

Intraindividual results from comparative metrics. **(a)** Mean signal in default mode network with mean signal in task positive network subtracted from its value. Instances faster than each individual's median reaction time are shown as dashed lines; instances slower than each individual's median reaction time are shown as solid lines. *X* axis is the amount of time between the calculated value and the change onset cue to perform the task (negative is before task, positive is succeeding task). Error bars are one standard error. **(b)** Pearson product-moment correlation coefficient (*r*) for 12.3 s square window between mean default mode network signal and mean task positive network signal. Instances faster than each individual's median reaction time are shown as dashed lines; instances slower than each individual's median reaction time are shown as solid lines. *X* axis is the amount of time between the calculated value and the change onset cue to perform the task (negative is before task, positive is succeeding task). Error bars are one standard error. Comparisons found to be significant include magnitude difference at −8 s to −4 s and correlation at −8 s to −6 s. They are demarcated as follows: *passes SGoF at 0.05; **passes SGoF at 0.01; ***passes SGoF at 0.005; †passes standard Bonferroni correction at 0.05.

Bonferroni correction: separating instances by overall median response time and using short-window correlation at peristimulus times of −12 s and −10 s (fast response greater negative correlation, $P = 4.59 \times 10^{-4}$, 3.28×10^{-4}).

For linear analysis, tests passing SGoF correction at 0.05 FWER included: magnitude difference at peristimulus times of −6 s and −4 s ($P = 2.11 \times 10^{-2}$, 9.69×10^{-3}, $R^2 = 4.43 \times 10^{-2}$, 5.52×10^{-2}, negative slope suggesting slower performance is related to lower default mode minus task positive) and at peristimulus times of 4 s to 8 s ($2.95 \times 10^{-3} \leq P \leq 2.42 \times 10^{-2}$, $4.38 \times 10^{-2} \leq R^2 \leq 7.56 \times 10^{-2}$, positive slope suggesting slower performance is related to greater default mode minus task positive) and using short-window correlation at peristimulus times of −12 s, −8 s to −2 s, 2 s, and 4 s ($1.23 \times 10^{-2} \leq P \leq 2.77 \times 10^{-2}$, $4.13 \times 10^{-2} \leq R^2 \leq 5.19 \times 10^{-2}$, positive slope suggesting slower performance is related to greater correlation). Significant results at negative peristimulus times for linear analysis but not two group analysis were in part due to that slow response instances followed a linear trend while fast response instances had high variance (Supporting Information Fig. S3).

Intraindividual Prediction Using Comparative Metrics

Figure 6 illustrates how comparative metrics relate to intraindividual performance at peristimulus times from 16 s before 24 s succeeding change onset. The first comparative metric is local difference in magnitude which is the signal in the task positive network subtracted from the signal in the default mode network at the peristimulus time around the instance; it is shown in Figure 6a. The second comparative metric is short-window correlation which is *r* in a 12.3-s window centered at the peristimulus time around the instance (Fig. 6b). Individual instances are separated into slow and fast response groups by each individual's own median response time, and the metrics from each group are plotted. Error bars are one standard error.

Unlike interindividual comparisons (Fig. 5), intraindividual comparisons (Fig. 6) isolate significant results to only peristimulus times before task performance.

Tests passing SGoF correction at 0.05 FWER included: using magnitude difference at peristimulus times of −8 s to −4 s (fast response greater positive difference indicating default mode signal was greater, $4.15 \times 10^{-3} \leq P \leq 1.21 \times 10^{-2}$), and using short-window correlation at peristimulus times of −8 s and −6 s (fast response greater negative correlation, $P = 8.78 \times 10^{-3}$, 1.03×10^{-2}).

Intraindividual Prediction Within Fast and Slow Groups

Figure 7 illustrates how comparative metrics relate to intraindividual performance at peristimulus times from −8

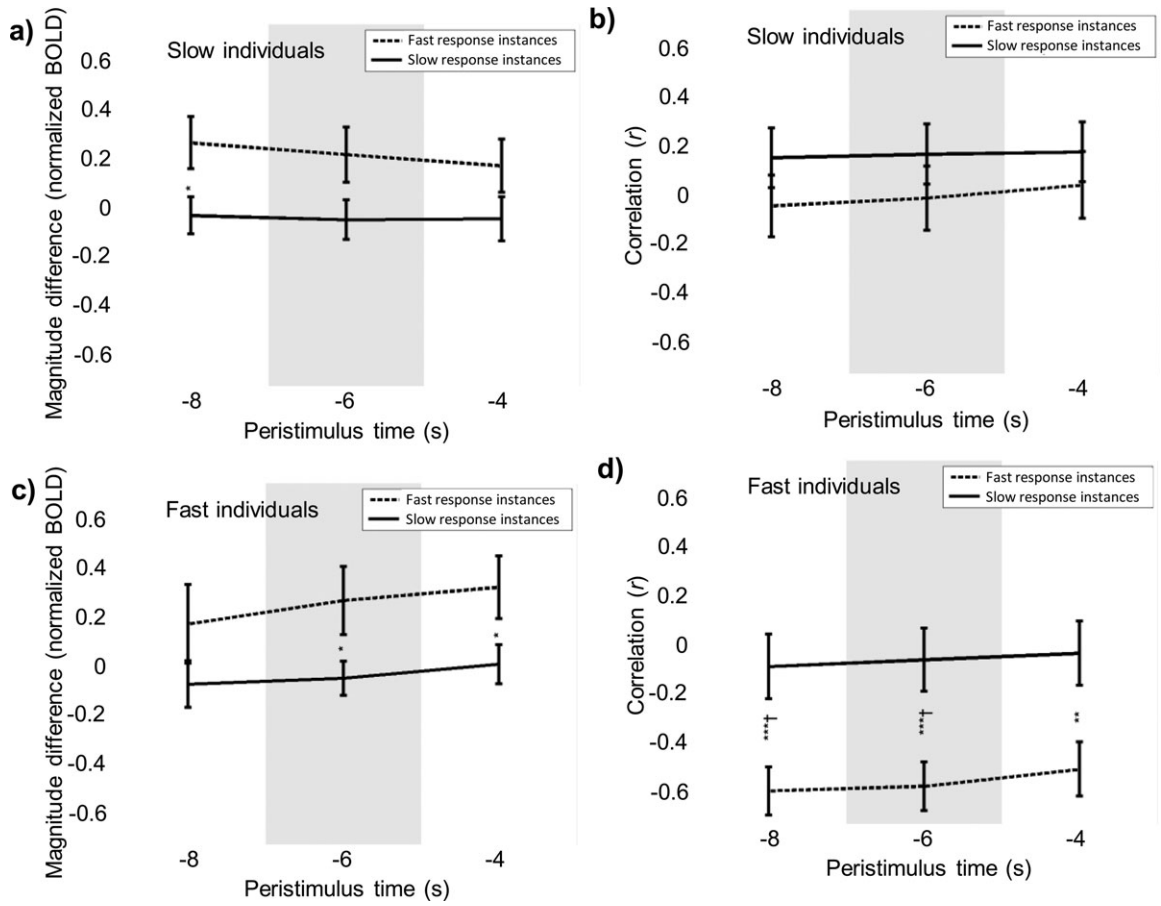

Figure 7.

Intraindividual results at previously significant peristimulus times for fast and slow groups. Peristimulus times of −8 s to −4 s are analyzed, as these were the only peristimulus times significant for intraindividual analysis. **(a)** Mean signal in default mode network with mean signal in task positive network subtracted from its value. Instances faster than each individual's median reaction time are shown as dashed lines; instances slower than each individual's median reaction time are shown as solid lines. *X* axis is the amount of time between the calculated value and the change onset cue to perform the task (negative is before task, positive is succeeding task). Error bars are one standard error. Only instances from individuals whose own median response time was above the overall median response time are used (slow individuals group). **(b)** Pearson product-moment correlation coefficient (*r*) for 12.3 s square window between mean default mode network signal and mean task positive network signal. Instances faster than each individual's median reaction time are shown as dashed lines; instances slower than each individual's median reaction time are shown as solid lines. *X* axis is the amount of time between the calculated value and the change onset cue to perform the task (negative is before task, positive is succeeding task). Error bars are one standard error. Only instances from individuals whose own median response time was above the overall median response time are used (slow individuals group). **(c)** As (a); except only instances from individuals whose own median response time was below the overall median response time are used (fast individuals group). **(d)** As (b); except only instances from individuals whose own median response time was below the overall median response time are used (fast individuals group). Comparisons found to be significant include magnitude difference at −8 s for slow individuals, and magnitude difference at −6 s and −4 s and correlation at −8 s to −4 s for fast individuals. They are demarcated as follows: *passes SGoF at 0.05; **passes SGoF at 0.01; ***passes SGoF at 0.005; †passes standard Bonferroni correction at 0.05.

s to −4 s, when fast and slow individuals are separated. These peristimulus times were chosen as these were the only points significant for prior intraindividual analysis (see −8 s to −4 s on Fig. 6). The first comparative metric is local difference in magnitude which is the signal in the task positive network subtracted from the signal in the default mode network at the peristimulus time around the instance (Fig. 7a,c). The second comparative metric is short window correlation which is *r* in a 12.3-s window centered at the peristimulus time around the instance (Fig. 7b,d).

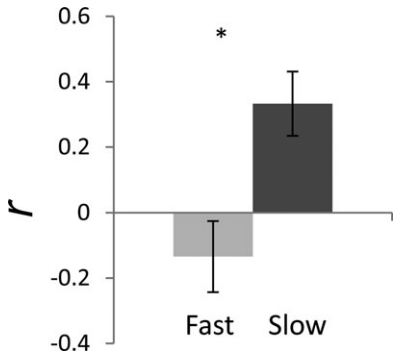

Figure 8.

Resting-state results. The Pearson product-moment correlation coefficient was calculated between the mean signal from the default mode network and the mean signal from the task positive network in each resting-state functional imaging run. The mean *r* is shown for (left) individuals whose own median response time was less than the overall median response time and (right) individuals whose own median response time was greater than the overall median response time. Error bars are one standard error. This difference was significant ($P = 6.05 \times 10^{-3}$).

Individuals are first separated into slow and fast groups first by the overall median response time, then individual instances within each group are subdivided into fast and slow response groups using each individual's own median response time. The metrics from each subgroup are plotted. Figure 7a,c is for the slow individuals group while Figure 7b,d is for the fast individuals group. Error bars are one standard error.

Tests passing SGoF correction at 0.05 FWER included: within the slow individuals group using magnitude difference at a peristimulus time of −8 s (fast response greater positive difference indicating default mode signal was greater, $P = 2.32 \times 10^{-2}$), within the fast individuals group using magnitude difference at peristimulus times of −6 s and −4 s (fast response greater positive difference indicating default mode signal was greater, $3.57 \times 10^{-2} \leq P \leq 3.70 \times 10^{-2}$) and within the fast individuals group using short-window correlation at peristimulus times of −8 s to −4 s (fast response greater negative correlation, $3.44 \times 10^{-3} \leq P \leq 9.65 \times 10^{-3}$).

Two tests passed Bonferroni correction within the fast individuals group. These were short-window correlation at peristimulus times of −8 s and −6 s (fast response greater negative correlation, $3.44 \times 10^{-3} \leq P \leq 4.39 \times 10^{-3}$).

In every case whether the mean value for fast instances was greater or less than the mean value for slow instances matched what was seen when the groups were combined (Fig. 6).

Resting-State Correlation

Using the traditional analysis method of correlation between networks on the time scale of entire resting-state functional imaging runs [Albert et al., 2009; Kelly et al., 2008; Tambini et al., 2010; Wang et al., 2010] a significant relationship was shown between faster reaction times and anticorrelation between the default mode and task positive networks (Fig. 8). This was similar to what was seen using short-window correlation (see InterIndividual Prediction Using Comparative Metrics above) and what has been observed in other attention-requiring tasks [Kelly et al., 2008].

The group of individuals with below median reaction times had mean negative correlation between their default mode network and task positive network (mean −0.134, standard deviation 0.408), and individuals with above median reaction times had mean positive correlation (mean 0.333, standard deviation 0.312). This difference was significant ($P = 6.05 \times 10^{-3}$).

No significant relationship was found between masks generated for fast performers versus slow performers, when the whole functional imaging run was used to generate the mask.

Control

No control tests included a *P* value that passed multiple comparisons correction by SGoF or Bonferroni at 0.05 FWER or below. Eight out of 10 experimental tests showed significant results at the 5% level. The likelihood of this result being a false positive is vanishingly small (1.61×10^{-9}%, from binomial distribution).

DISCUSSION

Summary of Results

All comparisons consistently demonstrated that a greater difference between the signal in the default mode network and the task positive network predicts faster performance on the PVT. The results from comparing the local difference in magnitude between the two networks suggested that this difference may be directional and bimodal, with greater signal in the default mode network sufficiently before the task associated with faster performance and greater signal in the task positive network during or after the task associated with faster performance (Figs. 5 and 6).

The relationship between task positive/default mode anticorrelation and fast reaction times is statistically strong and preserved across all time scales. The statistically strongest result (when all peristimulus times were considered) was when an overall median reaction time and correlation in 12.3 s windows was used (Fig. 5b). In the Supporting Information, network masks are also generated within 12.3 s windows (rather than entire functional imaging runs). As networks generated in short windows are likely to reflect temporary changes in network dynamics [Deco et al., 2011; Honey et al., 2007] these results do not

completely match the results from the main text. However, the statistically strongest result from the main text is similar even when using these temporary networks (Supporting Information Fig. S2bC). Therefore the result when only a 12.3-s window is considered for both network generation and correlation calculation largely matches the result when the whole functional imaging run is considered for these calculations (Fig. 8).

Using signal in a single network did not significantly predict PVT performance before the task, suggesting relative difference between networks may be more important than absolute signal within a single network (Supporting Information Fig. S1). The only significant relationships between signal and task performance were seen after the likely neural response to the task itself (Supporting Information Fig. S1b) and have already been documented in similar tasks [Chee et al., 2008; Prado et al., 2011].

Significant results were found at peristimulus times before task performance that suggest that speed of response on individual instances of the PVT can be predicted on an instance-by-instance basis for a specific individual, rather than only between different individuals. Significant prior differences in network state were seen using local difference in magnitude and correlation in a 12.3-s window for instances separated by each individual's own median reaction time (Fig. 6). However, a significant predictive difference was not seen when using local difference in magnitude and an overall median reaction time to separate instances (Fig. 5a) and could only be seen using linear regression, which had higher statistical power (Fig. 5c). While using an overall median or linear regression and correlation in a 12.3-s window shows similar results to using individuals' own medians at peristimulus times of 6 s to 8 s before the task, it also shows similar results at many other peristimulus times not present when medians are calculated separately (Fig. 5b,d).

While the majority of results agreed that a greater difference between the signal dynamics of the networks is required for optimal response times, two different time scales were observed. Results from resting-state correlation (Fig. 8), correlation within a 12.3-s window using an overall median response time (Fig. 5b) and local difference in magnitude using linear regression (Fig. 5c) all showed a persistent difference; this difference was significant for 15 out of 21 peristimulus times tested using windowed analysis (with an identical trend for the six non-significant results, Fig. 5b). However, if individual instances were separated into fast and slow groups based on individual median reaction times (so that each individual has approximately half of reaction times classified as fast and half as slow) the comparative metrics only showed a significant difference before the change onset within a comparatively small peristimulus time span (Fig. 6); significant results were isolated to 4 to 8 s before the change onset.

Further support for the existence of a second, shorter, time scale was that intraindividual prediction was possible even when the analysis only considered individuals who were generally fast or slow (Fig. 7). When individuals were separated into fast and slow groups, difference in magnitude was still significantly greater for comparatively faster response instances both for generally slow and generally fast responders (Fig. 7a,c). When only individuals classified as generally fast were used, correlation in a 12.3-s window was still significantly more negative for comparatively faster response instances (Fig. 7d). When only individuals classified as generally slow were used, the mean result for comparatively faster response instances was lower correlation, but the difference was not significant (Fig. 7b).

The Default Mode Network and Anticorrelation

Why does the brain have a default mode, and why would it fluctuate in an anticorrelated manner with regions associated with attention? One possible answer for the first part of this question, which was proposed by the initial work of Raichle et al. [2001], is that regions within the default mode network provide useful functions when a subject is at rest. They suggested that the precuneus may gather information and the medial frontal cortex may evaluate its salience. Both the present study's results, and previous work [Kelly et al., 2008; Prado and Weissman, 2011a), move us closer to answering the second part of the question (i.e., the purpose for the anticorrelated fluctuations). These studies have demonstrated that performance is optimized when the task-positive and default mode networks are anticorrelated and, conversely, coactivation of the task positive network and the default mode network is detrimental to performance. The mechanism by which anticorrelation results in improved performance requires further study; however, some possible answers have already been suggested. One possibility is that anticorrelation itself may not causally affect performance but instead serves as "an index of the degree of regulation of activity in those networks" [Kelly et al., 2008; p 528]; in this case anticorrelation is a biomarker of the underlying processes that regulate behavior. Another possibility is that activity within one functional network may interfere with initiation or sustenance of activity within a different functional network, such as the default mode network interfering during task performance [Eichele et al., 2008]. Anticorrelation creates a situation where cross-activation and hence cross-interference is unlikely.

How then can the brain ensure at least occasional activation of the default mode network, but also discourage coactivation between it and task positive regions? The spatiotemporal dynamics observed in studies by Grigg and Grady [2010] and Majeed et al. [2011] provide one potential hypothesis. Through repeated, dynamic alternation between default mode and task positive regions, the human brain can both activate the default mode network at some interval and also ensure these activations do not coincide with activations in the task positive network. The

present results thus support the importance of competition between the default mode and task positive functional networks to optimal performance [Kelly et al., 2008], but append the important result that this competition varies on a much smaller time scale than had been suspected based on interindividual studies, and that intraindividual behavioral prediction is possible. This time scale is consistent with the spatiotemporal dynamics which take approximately 10 to 20 s to switch between networks (Fig. 2 in Grigg and Grady, 2010; Fig. 5 in Majeed et al., 2011].

The present study used regression to remove the whole-brain signal before analysis. It has been demonstrated that this can potentially create artifactual deactivation resulting in artifactual anticorrelation [Gavrilescu et al., 2002]. However, recent work by Fox et al. [2009] demonstrated that the global signal in fMRI is not preferentially located, suggesting regression is unlikely to create artifactual networks; Fox et al. also demonstrated that observed anticorrelated networks are highly consistent, suggesting such networks cannot be attributed to global signal removal alone [Fox et al., 2009]. If anticorrelation was completely artifactual, the network driving behavior should be related to behavior itself; the relationship between the artifactual anticorrelated network and behavior should mimic the network driving behavior with opposite sign and greater noise. However, the present study does not support this; rather, before the task the amount of anticorrelation between networks was significantly related to behavior, whereas the inherent activity within a single network was not (compare Fig. 5 and Supporting Information Fig. S1). This supports Fox et al.'s hypothesis of a "biological basis to anticorrelated networks" [Fox et al., 2009; p 3280].

Correlation Within Entire Functional Imaging Runs Versus 12.3-s Windows

Few studies have examined resting-state correlation in short time windows; typically the entire fMRI run is used. Sakoglu et al. used 30 s windows in data from patients with schizophrenia as compared with normal controls to find greater diagnostic information than from whole functional imaging runs [Sakoglu et al., 2010]. Chang and Glover observed that the low frequency fluctuations which make up functional networks vary in terms of power and dominant frequency band over time [Chang and Glover, 2010]. A simulation of resting-state activity in the Macaque brain by Honey et al. [2007] demonstrated that functional networks gradually change over time if correlation in 30 s windows is used as opposed to entire simulated functional imaging runs. A recent review by Deco et al. [2011] also noted that, in such simulations, correlation coefficients vary based upon the window size used to perform analysis.

The results presented here suggest that the relationship seen in previous work between behavioral differences and entire-functional-imaging-run correlation [Kelly et al., 2008] may be a summation of global differences between individuals and numerous low-frequency yet second-scale processes, the latter of which can be examined on their original time scales of only a few seconds. Using the same overall median response times and same mask-generation methods as were used for resting-state analysis, the anticorrelation in fast instances was seen at peristimulus times both following and before the hypothesized hemodynamic response to neural activity (Fig. 5b); here about 4 s [Miezin et al., 2000]. The 12.3 s window was short enough such that it could not have contained a full cycle of the fastest fluctuation after filtering. Therefore, the anticorrelation which was related to fast responses could only have been based upon momentary differences between networks which can be characterized on a scale of seconds.

On an individual basis, the second-scale relationship between these two networks is also significantly related to behavior; however, at fewer peristimulus times. When each individual's own median was used to classify instances as fast or slow, the same effect was seen: greater anticorrelation predicts faster performance. However, in this case a significant effect was only seen at 6 s to 8 s before task performance (Fig. 6b).

Difference in Mean Signals

A mean signal in the default mode network greater than the mean signal in an anticorrelated network was significantly related to faster response times before task performance and slower response times following task performance (Figs. 5a and 6a). However the prior result was significant only if individuals' median reaction times were used and the latter significant only if an overall median reaction time was used. This may be due to intraindividual differences on an instance by instance basis being more predictive of the general waiting state needed to respond quickly: the intraindividual differences in mean occur at two out of three of the same peristimulus times as intraindividual differences in correlation between networks. Also, as the automatically generated anticorrelated networks include premotor regions (Figs. 2 and 3); a motor response that is similar in all individuals may occlude results unless a global median response time is used. Interestingly, the ideal (fast response) state for the difference in mean signals overall is alternation between networks at approximately 0.05 Hz, on the order of what has been observed in studies of spatiotemporal dynamics [Grigg and Grady, 2010; Majeed et al., 2011].

Comparison With Previous Research That Used Distracting Stimuli

The present study used the PVT. Other investigations into the effects of brain networks on attention have used other tasks, many of which include distracting stimuli. For example, in the flanker task, an individual must respond to a centrally presented target while ignoring surrounding

distracting symbols such as arrows or letters [Eriksen and Eriksen, 1974].

As the flanker task and the PVT both require an individual to attend to visual stimuli and react with motor movement, results from these tasks should be similar. However, as the flanker task is a two-choice task that involves inhibiting the effects of distracting stimuli, it may require more attentional control to selectively attend to the target location than the PVT. Thus the flanker task may be more reliant on functions associated with task positive brain regions such as inhibition and maintenance of attention [Fox et al., 2005; Fransson, 2005] while the PVT may be more reliant on function associated with default mode brain regions such as gathering of salient information [Raichle et al., 2001]. However there is no reason to believe that competition between networks [Kelly et al., 2008] would be desirable in either task, so anticorrelation between networks might be expected in both tasks.

Consistent with this prediction, it was demonstrated by Kelly et al. [2008] that an individual's ability to maintain an anticorrelated relationship between the default mode network and the task positive network predicted consistent reaction times on a flanker task, suggesting that maintenance of anticorrelation should improve performance. Our finding, that anticorrelation during the resting state predicts lower median response times, demonstrates that this idea extends to the PVT as well. In addition, using the short-window correlation metric, a significant difference was found between fast and slow instances on an intraindividual level for individuals classified as fast for resting-state analysis, but not for individuals classified as slow (Figs. 5b,d and 6b). This would suggest that individuals who perform optimally are better at modulating competition between networks as Kelly et al. suggested. However, Kelly et al. did not use correlation within windows, but rather maximal change inside 8 s windows to look for transient events; they were unable to relate these to performance. Using an even more time-localized method, local difference in magnitude, both overall fast and overall slow performers on the PVT did show significant differences between their fast and slow instances (Figs. 5a,c and 6a).

However, in the present study, the specific signal changes around each instance of task performance differ from what has been observed for the flanker task. Groundbreaking work by Weissman et al. [2006] demonstrated that fast performance on a visual letter-based task was associated with a prior reduction in the default mode network signal and increase in the task positive network signal. Eichele et al. followed the work of Weissman but used a standard arrow-based flanker task and focused on prediction of correct trials [Eichele et al., 2008]. They demonstrated that these predictive changes in signal maintain their directionality up to 30 s before the performance of the task after correcting the BOLD signal for the hemodynamic response delay.

In the present study, when an overall median value was used to separate response times, the default mode network signal was significantly lower than the anticorrelated network's signal at 6 s succeeding the task (neural electrical differences expected 2 s after task occurrence), following the peak of the hemodynamic response from motor regions [Miezin et al., 2000]. When individual median values were used to separate response times, the default mode network signal was significantly greater than the task positive network signal from 4 s to 8 s before the task; therefore peak neural electrical differences would be expected 8 s to 12 s prior [Miezin et al., 2000]. The first of these results was seen in the flanker task [Eichele et al., 2008; Weissman et al., 2006] and supports fMRI activation seen for the PVT by Drummond et al. [2005]. The present study's second result, where the default mode signal is greater before the task, is in the opposite direction of Eichele et al. and Weissman et al. The opposite result may be due to the flanker task requiring greater cognitive control, and thus more sustained activation of the task positive network. Another possibility is suggested by data that drowsiness both reduces performance on the PVT [Graw et al., 2004; Jewett et al., 1999] and was recently observed by Gular et al. [2009] to reduce the amount of signal change in the default mode. If individuals exhibit a range of drowsiness the loss of default mode may become a factor at some point sufficiently before task performance. Thus, it is also possible that individual drowsiness is a much greater risk in the PVT than the flanker task. As drowsiness was not systematically tested in the present experiment the exact relationship is unknown.

Comparing the present results with another recent study of an attention task [Prado and Weissman, 2011a) also suggests that comparisons between attention tasks are possible. Prado et al. used a task where subjects were required to attend to either auditory (spoken letters) or visual (displayed letters) stimuli and ignore letters in the other modality, which were either congruent or incongruent with the correct modality. They observed that greater connectivity between the precuneus (default mode) and dorsolateral prefrontal cortex (task positive) was linked to increased reaction time on the current trial but decreased reaction time on the succeeding trial. As Prado et al. calculated connectivity using psychophysiological interaction [Friston et al., 1997] and a hemodynamic response function with a peak at approximately 6 to 8 s [Josephs et al., 1997] their results are most comparable to the current study's local difference in magnitude using linear regression at positive peristimulus times of 6 s and 8 s (see Fig. 5c, peristimulus times of 6 s and 8 s). Even though the PVT is a less complicated task, the direction of the results (greater difference and greater anticorrelation are linked to faster performance) is identical.

A Critical Period for Intraindividual Task Performance?

As the intraindividual relationship between reaction time and network activity was limited to 4 to 8 s before

task performance (indicating neural activity 8 to 12 s prior) this suggests that intraindividual variation may influence studies where the time separation between trials falls within this window. This may have been seen in the present study. Using local difference in magnitude, two-group analysis did not show a significant relationship in interindividual analysis within the 4 to 8 s prior time span (Fig. 5a). However, with the increase in statistical power using linear regression, this difference in intraindividual performance was now seen interindividually (Fig. 5c).

Why does this critical period for intraindividual performance exist? Its leftmost bound (−8 s) may be determined by the fact that the neural mechanisms for task preparation may differ from those for task performance, as Prado et al. observed that effects detrimental for the current trial could enhance a future trial [Prado and Weissman, 2011a). Alternately it may be due to a lack of statistical power at long peristimulus times in the present study. Its rightmost bound (−4 s) may be determined by task interference from resting-state networks [Eichele et al., 2008; Weissman et al., 2006]. It is also possible that the time scale upon which spontaneous fluctuations affect behavior is slow enough so that from 8 s before the neural response itself (about 4 s succeeding) it isn't possible to resolve its effects.

Stimulus Detection Versus Speed of Response

Previous studies have shown a significant relationship between stimulus detection and signal within the default mode network and also within the dorsal attention system which contains many of the same brain regions as the task positive network such as the intraparietal sulcus and frontal eye field [compare Kelly et al., 2005 with Sadaghiani et al., 2009].

However, in the present study, no significant difference was found before task performance between fast instances and slow instances using individual networks (Supporting Information Fig. S1). It should be considered that, in the present study, there were not enough "miss" instances (instances of the PVT where individuals did not respond) to use in analysis (only 18 instances in the entire study were missed, these occurred in only four subjects). Therefore, every result analyzed can be considered a "hit" in terms of stimulus detection. The evolution over time of the mean signal in the default mode and task positive networks (Supporting Information Fig. S1a,c) appears bimodal, potentially similar to "hit" results seen by Sadaghiani et al. [2009] using auditory detection. However, in future studies the protocol would need to be changed to result in more "miss" instances for a comparative analysis to be done.

CONCLUSION

The results presented here extend previous results regarding network anticorrelation to rapid performance on the PVT. In addition to results that are comparable to previous studies, the present study suggests that the time scale at which anticorrelation between the default mode and task positive networks predicts improved performance is very small, at least as short as a 12.3-s window both inter and intraindividually, and potentially this opposing relationship can be seen to predict performance on an intraindividual basis at a single time point if one network's normalized signal is subtracted from the other (Fig. 6a). These results would allow researchers to use short windows to evaluate the current condition of functional networks without requiring long resting-state functional imaging runs.

The present study also suggests that predictive metrics resulting from spontaneous oscillations may reflect a combination of both intraindividual and interindividual variation in network properties. However, most previous studies have only considered either interindividual differences in spontaneous fluctuations or large scale interindividual network differences in resting-state networks. The simple method used in the present study to group instances by both intraindividual and interindividual differences, as well as using similar metrics for both resting-state data and instantaneous data, can be applied in future studies to better understand how both the individual's transient state and the individual themselves affect results.

The contribution of the global signal was simply regressed in this study [Murphy et al., 2009; Scholvinck et al., 2010], but for real-time performance prediction it remains an open problem. Results generated using network masks generated in 12.3-s windows (see Supporting Information) are a promising future direction, even if they are not expected to match results generated using more stable networks [Fig. 2 and Supporting Information Fig. S2, see also Deco et al., 2011]. However, the results presented here are, in general, promising for the future development of second-scale, real-time performance prediction using functional networks.

ACKNOWLEDGMENTS

The authors thank Waqas Majeed for his help with human data preprocessing, Antonio Carvajal Rodríguez for providing the Sequential Goodness of Fit software on the web at http://webs.uvigo.es/acraaj/SGoF.htm, and Matthew Sochor for providing the 2d rigid body registration for *MATLAB* software on the web at http://www.mathworks.com/matlabcentral/fileexchange/19086. This research was performed under an appointment to the U.S. Department of Homeland Security (DHS) Scholarship and Fellowship Program, administered by the Oak Ridge Institute for Science and Education (ORISE) through an interagency agreement between the U.S. Department of Energy (DOE) and DHS. ORISE is managed by Oak Ridge Associated Universities (ORAU) under DOE contract number DE-AC05-06OR23100. All opinions expressed in this

article are the author's and do not necessarily reflect the policies and views of DHS, DOE, or ORAU/ORISE. The authors also thank their two anonymous reviewers for numerous helpful suggestions including the suggestion to generate masks within the 12.3 s windows themselves.

REFERENCES

Albert NB, Robertson EM, Miall RC (2009): The resting human brain and motor learning. Curr Biol 19:1023–1027.

Biswal B, Yetkin FZ, Haughton VM, Hyde JS (1995): Functional connectivity in the motor cortex of resting human brain using echo-planar MRI. Magn Reson Med 34:537–541.

Boly M, Phillips C, Balteau E, Schnakers C, Degueldre C, Moonen G, Luxen A, Peigneux P, Faymonville ME, Maquet P, Laureys S (2008): Consciousness and cerebral baseline activity fluctuations. Hum Brain Mapp 29:868–874.

Brett M, Anton J, Valabregue R, Poline J (2002): Region of interest analysis using an SPM toolbox. In: Proceedings of the 8th International Conference on Functional Mapping of the Human Brain; June 2–6; Sendai, Japan.

Calhoun VD, Adali T, Pearlson GD, Pekar JJ (2001): Spatial and temporal independent component analysis of functional MRI data containing a pair of task-related waveforms. Hum Brain Mapp 13:43–53.

Carvajal-Rodriguez A, de Una-Alvarez J, Rolan-Alvarez E (2009): A new multitest correction (SGoF) that increases its statistical power when increasing the number of tests. BMC Bioinformatics 10:209.

Chang C, Glover GH (2010): Time-frequency dynamics of resting-state brain connectivity measured with fMRI. Neuroimage 50:81–98.

Chee MW, Tan JC, Zheng H, Parimal S, Weissman DH, Zagorodnov V, Dinges DF (2008): Lapsing during sleep deprivation is associated with distributed changes in brain activation. J Neurosci 28:5519–5528.

Cordes D, Haughton VM, Arfanakis K, Wendt GJ, Turski PA, Moritz CH, Quigley MA, Meyerand ME (2000): Mapping functionally related regions of brain with functional connectivity MR imaging. AJNR Am J Neuroradiol 21:1636–1644.

Deco G, Jirsa VK, McIntosh AR (2011): Emerging concepts for the dynamical organization of resting-state activity in the brain. Nat Rev Neurosci 12:43–56.

Dinges DF, Powell JW (1985): Microcomputer analyses of performance on a portable, simple visual Rt task during sustained operations. Behav Res Methods Instrum Comput 17:652–655.

Drummond SP, Bischoff-Grethe A, Dinges DF, Ayalon L, Mednick SC, Meloy MJ (2005): The neural basis of the psychomotor vigilance task. Sleep 28:1059–1068.

Eichele T, Debener S, Calhoun VD, Specht K, Engel AK, Hugdahl K, von Cramon DY, Ullsperger M (2008): Prediction of human errors by maladaptive changes in event-related brain networks. Proc Natl Acad Sci USA 105:6173–6178.

Eriksen BA, Eriksen CW (1974): Effects of noise letters upon identification of a target letter in a nonsearch task. Percept Psychophys 16:143–149.

Fox MD, Corbetta M, Snyder AZ, Vincent JL, Raichle ME (2006): Spontaneous neuronal activity distinguishes human dorsal and ventral attention systems. Proc Natl Acad Sci USA 103:10046–10051.

Fox MD, Snyder AZ, Vincent JL, Corbetta M, Van Essen DC, Raichle ME (2005): The human brain is intrinsically organized into dynamic, anticorrelated functional networks. Proc Natl Acad Sci USA 102:9673–9678.

Fox MD, Zhang DY, Snyder AZ, Raichle ME (2009): The global signal and observed anticorrelated resting state brain networks. J Neurophysiol 101:3270–3283.

Fransson P (2005): Spontaneous low-frequency BOLD signal fluctuations: An fMRI investigation of the resting-state default mode of brain function hypothesis. Hum Brain Mapp 26:15–29.

Friston KJ, Buechel C, Fink GR, Morris J, Rolls E, Dolan RJ (1997): Psychophysiological and modulatory interactions in neuroimaging. Neuroimage 6:218–229.

Gavrilescu M, Shaw ME, Stuart GW, Eckersley P, Svalbe ID, Egan GF (2002): Simulation of the effects of global normalization procedures in functional MRI. Neuroimage 17:532–542.

Graw P, Krauchi K, Knoblauch V, Wirz-Justice A, Cajochen C (2004): Circadian and wake-dependent modulation of fastest and slowest reaction times during the psychomotor vigilance task. Physiol Behav 80:695–701.

Greicius MD, Srivastava G, Reiss AL, Menon V (2004): Default-mode network activity distinguishes Alzheimer's disease from healthy aging: Evidence from functional MRI. Proc Natl Acad Sci USA 101:4637–4642.

Grigg O, Grady CL (2010): Task-related effects on the temporal and spatial dynamics of resting-state functional connectivity in the default network. PLoS One 5:e13311.

Gujar N, Yoo SS, Hu P, Walker MP (2009): The unrested resting brain: Sleep deprivation alters activity within the default-mode network. J Cogn Neurosci 22:1637–1648.

Hampson M, Driesen NR, Skudlarski P, Gore JC, Constable RT (2006): Brain connectivity related to working memory performance. J Neurosci 26:13338–13343.

Hampson M, Peterson BS, Skudlarski P, Gatenby JC, Gore JC (2002): Detection of functional connectivity using temporal correlations in MR images. Hum Brain Mapp 15:247–262.

Hasson U, Nusbaum HC, Small SL (2009): Task-dependent organization of brain regions active during rest. Proc Natl Acad Sci USA 106:10841–10846.

Honey CJ, Kotter R, Breakspear M, Sporns O (2007): Network structure of cerebral cortex shapes functional connectivity on multiple time scales. Proc Natl Acad Sci USA 104:10240–10245.

Jewett ME, Dijk DJ, Kronauer RE, Dinges DF (1999): Dose-response relationship between sleep duration and human psychomotor vigilance and subjective alertness. Sleep 22:171–179.

Josephs O, Turner R, Friston K (1997): Event-related f MRI. Hum Brain Mapp 5:243–248.

Kelly AM, Uddin LQ, Biswal BB, Castellanos FX, Milham MP (2008): Competition between functional brain networks mediates behavioral variability. Neuroimage 39:527–537.

Lim J, Dinges DF (2008): Sleep deprivation and vigilant attention. Ann NY Acad Sci 1129:305–322.

Logothetis NK, Murayama Y, Augath M, Steffen T, Werner J, Oeltermann A (2009): How not to study spontaneous activity. Neuroimage 45:1080–1089.

Majeed W, Magnuson M, Hasenkamp W, Schwarb H, Schumacher EH, Barsalou L, Keilholz SD (2011): Spatiotemporal dynamics of low frequency BOLD fluctuations in rats and humans. Neuroimage 54:1140–1150.

Miezin FM, Maccotta L, Ollinger JM, Petersen SE, Buckner RL (2000): Characterizing the hemodynamic response: Effects of presentation rate, sampling procedure, and the possibility of ordering brain activity based on relative timing. Neuroimage 11:735–759.

Murphy K, Birn RM, Handwerker DA, Jones TB, Bandettini PA (2009): The impact of global signal regression on resting state correlations: Are anti-correlated networks introduced? Neuroimage 44:893–905.

Prado J, Carp J, Weissman DH (2011): Variations of response time in a selective attention task are linked to variations of functional connectivity in the attentional network. Neuroimage 54:541–549.

Prado J, Weissman DH (2011a): Heightened interactions between a key default-mode region and a key task-positive region are linked to suboptimal current performance but to enhanced future performance. Neuroimage 56:2276–2282.

Prado J, Weissman DH (2011b): Spatial attention influences trial-by-trial relationships between response time and functional connectivity in the visual cortex. Neuroimage 54:465–473.

Raichle ME, MacLeod AM, Snyder AZ, Powers WJ, Gusnard DA, Shulman GL (2001): A default mode of brain function. Proc Natl Acad Sci USA 98:676–682.

Rombouts SA, Barkhof F, Goekoop R, Stam CJ, Scheltens P (2005): Altered resting state networks in mild cognitive impairment and mild Alzheimer's disease: An fMRI study. Hum Brain Mapp 26:231–239.

Sadaghiani S, Hesselmann G, Friston KJ, Kleinschmidt A (2010): The relation of ongoing brain activity, evoked neural responses, and cognition. Front Syst Neurosci 4:20.

Sadaghiani S, Hesselmann G, Kleinschmidt A (2009): Distributed and antagonistic contributions of ongoing activity fluctuations to auditory stimulus detection. J Neurosci 29:13410–13417.

Sakoglu U, Pearlson GD, Kiehl KA, Wang YM, Michael AM, Calhoun VD (2010): A method for evaluating dynamic functional network connectivity and task-modulation: application to schizophrenia. Magma 23:351–366.

Scholvinck ML, Maier A, Ye FQ, Duyn JH, Leopold DA (2010): Neural basis of global resting-state fMRI activity. Proc Natl Acad Sci USA 107:10238–10243.

Seeley WW, Menon V, Schatzberg AF, Keller J, Glover GH, Kenna H, Reiss AL, Greicius MD (2007): Dissociable intrinsic connectivity networks for salience processing and executive control. J Neurosci 27:2349–2356.

Shmuel A, Leopold DA (2008): Neuronal correlates of spontaneous fluctuations in fMRI signals in monkey visual cortex: Implications for functional connectivity at rest. Hum Brain Mapp 29:751–761.

Singh KD, Fawcett IP (2008): Transient and linearly graded deactivation of the human default-mode network by a visual detection task. Neuroimage 41:100–112.

Tambini A, Ketz N, Davachi L (2010): Enhanced brain correlations during rest are related to memory for recent experiences. Neuron 65:280–290.

Waites AB, Stanislavsky A, Abbott DF, Jackson GD (2005): Effect of prior cognitive state on resting state networks measured with functional connectivity. Hum Brain Mapp 24:59–68.

Wang L, Laviolette P, O'Keefe K, Putcha D, Bakkour A, Van Dijk KR, Pihlajamaki M, Dickerson BC, Sperling RA (2010): Intrinsic connectivity between the hippocampus and posteromedial cortex predicts memory performance in cognitively intact older individuals. Neuroimage 51:910–917.

Weissman DH, Roberts KC, Visscher KM, Woldorff MG (2006): The neural bases of momentary lapses in attention. Nat Neurosci 9:971–978.